Evaluation of oxygen isotope experiments on Pr-, Ca-, and Zn-substituted $YBa_2Cu_3O_7$

G. Soerensen and S. Gygax
Department of Physics, Simon Fraser University, Burnaby, British Columbia, Canada V5A 1S6
(Received 6 September 1994; revised manuscript received 12 December 1994)

The oxygen isotope effect measurements on $YBa_2Cu_3O_7$ substituted with Pr, Ca, and Zn, which were reported earlier, have been analyzed in detail to examine the validity of the large increases in the isotope coefficient at low critical temperatures. We find that for Pr and Pr:Ca substitutions there is a correlation between the isotope shift and the width of the transition. This suggests that the upturn in the isotope coefficient for Pr substitutions could be due, at least partially, to a sample quality problem. Furthermore, we show that for low-T_c sample pairs incomplete magnetic transitions introduce very large uncertainties. This was a problem particularly for the Zn-substitution series. We also point out that a linear extrapolation to 100% ^{18}O substitution results in an overestimate of the isotope coefficient.

INTRODUCTION

The existence of an oxygen isotope effect in $YBa_2Cu_3O_7$ much smaller than expected for a BCS-type superconductor is now well established.[1] This result has been widely used in arguments that a mechanism other than an electron-phonon interaction must be dominant in this and other high-temperature metal oxide superconductors. However, the discovery[2] that large isotope effects in $La_{2-x}Sr_xCuO_4$ can be achieved with Sr doping has renewed interest in isotope effect measurements. A recent article[3] summarizes the present experimental status in this field. It is shown that, as the maximum T_c of a compound is depressed by substitutions, the oxygen isotope effect increases and reaches large values. It is, however, far from certain that these large increases are not due in large part to material problems and experimental difficulties. In a series of articles and conference reports[4] we reported on the oxygen isotope effect in $YBa_2Cu_3O_7$ variously substituted with Pr, Ca, and Zn. Here we have now taken a critical second look at our earlier measurements to arrive at credible values for the isotope coefficient in these substituted materials.

We first summarize the preparation and characterization of our samples and discuss the details of how the measurements were obtained. We will then describe how we have defined the critical temperature and the isotope shift for the resistive and magnetic transitions and present the procedure for the determination of the transition width and the establishment of realistic uncertainties in critical temperatures and isotope shifts. This analysis goes well beyond the initial presentation contained in our earlier publications. In particular, we have given special attention to the samples with high concentrations of Pr and Zn which have low T_c's. In the case of Pr and Pr:Ca substitutions we find a clear correlation between the isotope shift and the width of the transition which leads us to conclude that the upturn of the isotope coefficient at low T_c is most likely smaller in ideal samples than what we observed in materials made in the customary way. No such correlation was observed for the Zn substitutions where the transition width remains small down to very low T_c values. We do find, however, that the samples with high Zn concentrations have incomplete magnetic transitions, although the resistance does go to zero within the resolution of the measurement. We will argue that this makes the determination of an isotope shift from magnetic transitions of such samples very inaccurate and we now reject these data points. We will also point out that resistively determined isotope shifts in samples that are only marginally superconducting could also be suspect. A summary of the result of our analysis is given at the end. In its graphic form (Fig. 12) it shows the variation of the isotope shift and the isotope coefficient as a function of the critical temperature for all three substitutional compounds. The observed isotope shifts follow quite closely the T_c dependence described in our earlier reports except for the high concentration Pr and Zn substitutions.

SAMPLE PREPARATION AND CHARACTERIZATION

Information about the preparation and characterization of our samples have been given in some detail in our previous publications.[4] They were prepared as polycrystalline ceramic pellets, because the gaseous exchange of ^{16}O with ^{18}O requires that the sample be fine grained and porous enough to allow the oxygen to fully penetrate into the sample. All the samples were prepared at the University of Alberta, from high purity oxides and carbonates. For each different concentration, the powder was placed in an alumina crucible for the calcination process. Following calcination, the powders were pressed into pellets and then placed in a parallel processing system for sintering as described elsewhere.[1]

The calcination and sintering procedures for the three different sets of substitutions are somewhat different and were designed to obtain good single phase material (calcinating) that is fully oxygenated (sintering process) with the appropriate isotope. The preparation method of the substitutions of 5 to 25 % Ca into $Y_{0.8}Pr_{0.2}Ba_2Cu_3O_{7-\delta}$ is different from the Pr-substituted samples and thus a 0% Ca-substituted sample is included as a comparison to the previous set of measurements.

The early magnetic measurements on the $(Y_{1-x}Pr_x)Ba_2Cu_3O_{7-\delta}$ system were done on small flakes broken off from the pellets. For the other groups (Pr, Pr:Ca substitutions, and Zn substitution), two pieces were cut from the pellets and shaped: a flat thin bar (0.6 mm×1 mm×6 mm) for resistivity measurements and a roughly cylindrical rod (1 mm diam×6 mm long) for magnetic measurements. The remaining pieces were used for Raman spectroscopy and to obtain the oxygen stoichiometry via secondary ion-mass spectroscopy (SIMS) measurement. The ceramic pellets are quite hard and difficult to cut. They were mounted on glass slides with a low melting point adhesive that is soluble in acetone. The samples were then slowly cut with a band saw that utilizes a diamond blade. In order to keep the sample from overheating, the saw blade and sample were kept cool by spraying the blade at the entry point to the sample with methanol from a squeeze bottle. The two desired pieces are then mounted (individually) on an aluminum polishing jig and polished on No. 600 grit sandpaper to give flat surfaces. In the case of the rod, all four faces were done and the corners were rounded with a small file and sandpaper to remove sharp edges. Because of the heating involved in mounting and polishing the samples, the heat created during cutting, the use of acetone to dissolve the adhesive, and the use of methanol in cooling the sample during cutting, it is possible that this sample shaping procedure could affect the critical temperature. Prior to the sample shaping, four-probe resistance measurements were performed on the pellets to provide a comparison for the resistivity measurements carried out on the bars. The resistivity curves, however, are in general no different than the resistance curves. Thus this method for sample shaping appears to have little, if any, effect on the sample characteristics.

The orthorhombic structure of the samples was

TABLE I. The $(Y_{1-x}Pr_x)Ba_2Cu_3O_{7-\delta}$ system. Critical temperature T_c of the ^{16}O samples with uncertainties; isotope shift ΔT_c, and isotope coefficient α extrapolated to 100% ^{18}O content. The ^{18}O concentration was determined by SIMS.

Pr x	^{18}O (%)	Method	T_c (^{16}O) (K)	ΔT_c (K)	α (@ 100% ^{18}O)
0.2	84.6	Magn.	$74.6^{+6.2}_{-0.2}$	0.69±0.02	$0.093^{+0.005}_{-0.01}$
0.2	84.6	Susc.	$74.9^{+5.9}_{-0.2}$	0.67±0.02	$0.090^{+0.005}_{-0.01}$
0.2	84.6	Res.	$75.5^{+0.2}_{-0.2}$	0.80±0.02	$0.11^{+0.005}_{-0.005}$
0.3	79.0	Magn.	$59.5^{+9.7}_{-0.2}$	1.33±0.14	$0.24^{+0.03}_{-0.06}$
0.3	79.0	Susc.	$59.6^{+9.7}_{-0.2}$	1.31±0.20	$0.24^{+0.04}_{-0.06}$
0.3	79.0	Res.	$60.5^{+0.5}_{-0.4}$	1.05±0.02	$0.19^{+0.005}_{-0.005}$
0.4	85.5	Magn.	$44.2^{+20.4}_{-0.2}$	1.71±0.15	$0.39^{+0.04}_{-0.14}$
0.4	85.5	Susc.	$45.8^{+16.3}_{-0.2}$	1.47±0.33	$0.32^{+0.08}_{-0.14}$
0.4	85.5	Res.	$47.0^{+0.7}_{-1.0}$	1.46±0.02	$0.31^{+0.01}_{-0.01}$
0.5	85.9	Susc.	$27.7^{+17.2}_{-0.2}$	2.14±0.25	$0.79^{+0.10}_{-0.37}$
0.5	85.9	Res.	$32.7^{+0.5}_{-1.7}$	1.66±0.02	$0.51^{+0.04}_{-0.01}$

TABLE II. The $(Y_{1-x-y}Pr_xCa_y)Ba_2Cu_3O_{7-\delta}$ system. Critical temperature T_c of the ^{16}O samples with uncertainties; isotope shift ΔT_c, and isotope coefficient α extrapolated to 100% ^{18}O content. The ^{18}O concentration was determined by SIMS.

Pr x	Ca y	^{18}O (%)	Method	T_c (^{16}O) (K)	ΔT_c (K)	α (@ 100% ^{18}O)
0.2	0	85.0	Magn.	$71.0^{+5.0}_{-0.2}$	0.99±0.06	$0.14^{+0.01}_{-0.02}$
0.2	0	85.0	Susc.	$67.5^{+5.0}_{-2.0}$	0.97±0.01	$0.14^{+0.01}_{-0.01}$
0.2	0	85.0	Res.	$67.7^{+0.3}_{-0.3}$	0.97±0.03	0.14±0.01
0.2	0.05	84.0	Magn.	$62.9^{+2.3}_{-0.2}$	0.60±0.05	0.08±0.01
0.2	0.05	84.0	Susc.	$63.0^{+2.0}_{-0.2}$	0.57±0.06	0.08±0.01
0.2	0.05	84.0	Res.	$60.2^{+0.1}_{-0.1}$	0.60±0.08	0.08±0.01
0.2	0.1	78.0	Magn.	$54.7^{+1.6}_{-0.2}$	0.66±0.03	0.10±0.01
0.2	0.1	78.0	Susc.	$55.4^{+1.3}_{-0.2}$	0.66±0.02	0.09±0.01
0.2	0.1	78.0	Res.	$58.0^{+0.1}_{-0.3}$	1.00±0.01	0.15±0.01
0.2	0.15	77.0	Magn.	$38.1^{+1.0}_{-0.2}$	0.33±0.02	0.05±0.01
0.2	0.15	77.0	Susc.	$38.5^{+0.6}_{-0.2}$	0.32±0.10	$0.05^{+0.01}_{-0.02}$
0.2	0.15	77.0	Res.	$39.3^{+0.1}_{-0.1}$	0.49±0.01	0.07±0.005
0.2	0.2	76.0	Magn.	$28.6^{+1.1}_{-0.2}$	0.46±0.04	0.07±0.01
0.2	0.2	76.0	Susc.	$29.4^{+1.0}_{-0.2}$	0.48±0.01	0.08±0.01
0.2	0.2	76.0	Res.	$29.9^{+0.1}_{-0.2}$	0.57±0.005	0.09±0.005
0.2	0.25	75.0	Magn.	$18.1^{+1.0}_{-0.2}$	0.36±0.04	0.06±0.01
0.2	0.25	75.0	Susc.	$19.1^{+1.1}_{-0.2}$	0.37±0.03	0.06±0.01
0.2	0.25	75.0	Res.	$20.2^{+0.1}_{-0.7}$	0.59±0.05	0.10±0.01

confirmed via x-ray measurements utilizing the Cu $K\alpha$ Bragg diffraction peaks. The lattice constants obtained agree well with the accepted values. The effect of the increasing Pr substitution was a small linear increase in the lattice constants. There was no observable effect on the lattice parameters for the Zn and Ca substitutions. All the observed peaks can be accounted for. The main impurity for the Pr and Ca substitutions was $BaCuO_2$, whose signature is a triple peak in the range $2\Theta = 27°$ to 30°. We estimate that the concentration of this impurity phase amounts to less than 3%. The other impurity phases one might expect are $Y_2Cu_2O_5$ and CuO but the absence of such lines in our spectra rules out their presence. The formation of $BaCuO_2$ in the calcination/sintering process could be due to a small fraction of Pr ending up on Cu(2) sites. For a 20% Pr substitution we then explored nominal compositions of the type $(Y_{0.8-x}Pr_{0.2})Ba_{2-x}Cu_3O_7$ in an effort to make samples which are free of $BaCuO_2$. However, this was not successful and the samples were no better than those starting from stoichiometrically correct mixtures. The later samples, the Zn substitutions, did not show any impurity phases at the x-ray detection level.

There are three main frequency bands associated with the phonons that originate from oxygen vibrations in the $YBa_2Cu_3O_7$ system. They are accessible to Raman measurements and are generally accepted to be due to (1) an out-of-phase vertical (c axis) displacement of the Cu-O plane oxygen ions O(2) and O(3) at 340 cm^{-1}; (2) an in-phase vibration mode of O(2) and O(3) at 430 cm^{-1} and (3) an axial stretch mode of the Cu-O chain site O(4) atom at 500 cm^{-1}. Far-infrared reflectivity measurements along with Raman measurements reveal that all the oxygen active frequencies measured shifted to a lower value when ^{18}O is substituted for ^{16}O. Thus the observation of a decrease in the frequency shift for all three modes in isotope substitution measurements gives better site specific evidence that substitution has taken place than measurements by weight change or SIMS analysis. The shift of these phonon modes with the substitution of ^{18}O for ^{16}O, expected[5] to be 5.0%, is in good agreement with measurements done on some of our samples. A ra-

TABLE III. The $YBa_2(Cu_{1-z}Zn_z)_3O_{7-\delta}$ system. Critical temperature T_c of the ^{16}O samples with uncertainties; isotope shift ΔT_c, and isotope coefficient α extrapolated to 100 ^{18}O content. The ^{18}O concentration was determined by SIMS.

Zn z	^{18}O (%)	Method	T_c (^{16}O) (K)	ΔT_c (K)	α (@ 100% ^{18}O)
0.02	92	Magn.	$67.6^{+0.9}_{-0.3}$	0.26±0.07	0.03±0.01
0.02	92	Susc.	$67.5^{+1.0}_{-0.2}$	0.31±0.08	0.04±0.01
0.02	92	Res.	$67.7^{+0.6}_{-1.2}$	0.71±0.06	0.09±0.01
0.025	(92)	Magn.	$62.9^{+0.5}_{-0.2}$	0.26±0.03	0.04±0.01
0.025	(92)	Susc.	$63.0^{+0.7}_{-0.2}$	0.29±0.03	0.04±0.01
0.025	(92)	Res.	$60.2^{+3.0}_{-5.0}$	0.44±0.09	0.06±0.02
0.04	92	Magn.	$54.7^{+2.2}_{-0.3}$	0.41±0.07	0.07±0.01
0.04	92	Susc.	$55.4^{+1.2}_{-0.4}$	0.43±0.09	0.07±0.02
0.04	92	Res.	$58.0^{+0.7}_{-0.4}$	0.44±0.04	0.06±0.01
0.05	92	Magn.	$38.1^{+1.5}_{-0.2}$	0.12±0.05	0.03±0.01
0.05	92	Susc.	$38.5^{+1.2}_{-0.2}$	0.08±0.04	0.02±0.01
0.05	92	Res.	$39.3^{+0.5}_{-0.2}$	0.20±0.05	0.04±0.01
0.06	(92)	Magn.	$28.6^{+2.7}_{-0.2}$	0.29±0.03	0.09±0.01
0.06	(92)	Susc.	$29.4^{+1.6}_{-0.2}$	0.29±0.04	0.09±0.01
0.06	(92)	Res.	$29.9^{+0.8}_{-0.3}$	0.22±0.02	0.06±0.01
0.07	86	Magn	$18.1^{+3.3}_{-0.2}$	0.21±0.05	$0.11^{+0.03}_{-0.04}$
0.07	86	Susc.	$19.1^{+2.7}_{-0.2}$	0.23±0.02	$0.12^{+0.01}_{-0.03}$
0.07	86	Res.	$20.2^{+1.1}_{-0.7}$	0.34±0.02	0.14±0.02
0.075	88	Magn.	$11.5^{+3.0}_{-0.2}$	0.23±0.09	0.23±0.01
0.075	88	Susc.	$12.7^{+2.1}_{-0.2}$	0.17±0.05	$0.13^{+0.04}_{-0.05}$
0.075	88	Res.	$13.4^{+1.4}_{-0.2}$	0.29±0.01	$0.19^{+0.01}_{-0.03}$
0.08	(92)	Magn.	$8.5^{+3.3}_{-0.2}$	0.58±0.04	$0.65^{+0.06}_{-0.22}$
0.08	(92)	Res.	$9.6^{+1.5}_{-0.6}$	0.76±0.06	$0.70^{+0.11}_{-0.15}$
0.085	92	Res.	$5.7^{+1.4}_{-0.4}$	0.22±0.03	$0.34^{+0.08}_{-0.15}$
0.0875	92	Res.	$8.0^{+1.5}_{-0.5}$	0.25±0.05	$0.27^{+0.08}_{-0.09}$

man investigation[6] on the homogeneity of the oxygen substitution indicates that the apical oxygen site was not as completely substituted as were the O(2) and O(3) sites. From SIMS it was determined that the oxygen substitution was on average about 85% complete.

The oxygen content for the Zn-substituted samples was determined by iodometric titration (University of Alberta). There was little change in the oxygen stoichiometry, varying from 6.92 ± 0.03 to a maximum of 6.94 ± 0.03. The oxygen stoichiometry is thus not likely to be a factor in any of the measurements. The extent of the ^{18}O substitution is obtained from SIMS measurements (and by weighing for the Zn-substituted samples) and is reported in Tables I–III. Generally, the concentration of atomic ^{18}O, which is indicative of the completeness of the substitution, is in the range of 75 to 92 %. To obtain an isotope coefficient α at 100% ^{18}O substitution, a linear extrapolation was used. The validity of such an assumption is quite debatable. The effect would only be linear if all oxygen sites were substituted to the same degree and if all oxygen sites play similar roles in the mechanism for superconductivity. But a recent site-selective oxygen isotope study[7] on $YBa_2Cu_3O_{7-\delta}$ has revealed that more than 80% of the isotope effect is associated with the copper oxide planes. Raman measurements have shown that the apical oxygen sites O(4) is more difficult to substitute than the other oxygen sites.[5] It has also been shown[8] that increasing the Pr concentration leads to an increase in the Ba-O(4) distance, as well as an increase in the c-axis O(4) vibration frequency. This mode shows a strong electron-phonon interaction[9] and the localization of holes about the Ba is then strongly dependent on the Ba-O(4) distance. Thus the isotope substitution of oxygen at the O(4) site may affect the amount of localization of holes around Ba and hence the critical temperature and the isotope shift. A linear extrapolation to 100% ^{18}O will at least give an upper limit on the isotope coefficient α.

EXPERIMENTAL DETAILS AND DETERMINATION OF THE ISOTOPE SHIFT

The oxygen isotope effect in superconductors has been defined traditionally by $\alpha=-(\Delta \ln T_c)/(\Delta \ln M)$. In the case where there is more than one element with mass M_i, each will have its own isotope coefficient $\alpha_i=-(\Delta \ln T_c)/(\Delta \ln M_i)$, with a total isotope exponent defined as $\alpha_{\text{tot}}=\Sigma\alpha_i$. In the case of the fully oxygenated $YBa_2Cu_3O_{7-\delta}$ only the oxygen is found to produce a measurable isotope effect. For oxygen-deficient $YBa_2Cu_3O_{7-\delta}$, however, a large and negative Cu isotope effect is observed.[10] Setting $\Delta T_c=T_c(^{16}O)-T_c(^{18}O)$ gives $\alpha=[\ln(1-\Delta T_c/T_c)]/\ln 1.125$, where T_c is the critical temperature of the ^{16}O sample. Therefore, measuring the oxygen isotope effect involves measuring the critical temperature of the ^{16}O samples, T_c, and the shift in the critical temperature for the ^{18}O samples, ΔT_c.

We determine the critical temperature of the superconductors and its isotope shift from measurements of resistance and magnetic properties—dc magnetization and ac susceptibility. The resistivity of the samples was measured by a dc four-probe method where the current was reversed and the mean of the measuring voltage was recorded. Current densities were on the order of 0.2 A/cm^2. The low-field magnetic measurements, dc magnetization and ac susceptibility, were performed using a high sensitivity noncommercial, superconducting quantum interference device magnetometer. The instrument has no moving parts. Instead, the changing flux through a small pair of astatically wound pick-up loops consist of very thin coils of 7 turns each, 0.8 mm long and 5 mm in diameter whereas the samples in this investigation were either small flakes or roughly cylindrically shaped rods, 6 mm long and 1 mm in diameter. The signal is therefore dependent on the sample shape and must include return-flux corrections[11] if absolute magnitudes are desired.

dc and ac magnetic fields were applied simultaneously. A typical amplitude for dc magnetization measurements was 0.05 Oe, while the ac field at 160 Hz was usually orders of magnitudes smaller than this. A μ-metal shield around the dewar and a Pb shield inside it provide a residual field of the order of 1 mOe. The magnetic measurements were normally done as zero-field-cooled (ZFC) transitions which reflect the shielding properties of the ceramic samples. The field-cooled (FC) transitions which reflect the Meissner effect and pinning properties were also investigated. Since we are interested in the shift in critical temperature we concentrate our analysis on the temperature region where a diamagnetic signal first appears. This region is, for all our samples, within the reversibility range where ZFC and FC transitions coincide. We therefore concentrate on the ZFC transitions and usually normalize the measurements to the full diamagnetic shielding signal. However, this is only meaningful if the T_c of the sample is not to close to 4.2 K. Otherwise only partial shielding might occur. We discuss this problem at the appropriate place.

For the magnetic measurements the samples were attached to the end of a sapphire rod with Apiezon N grease. The sapphire rod, 5.5 cm long and 3.8 mm in diameter, is attached to a copper block containing a heater and calibrated carbon-glass thermometer. A temperature difference between sample and thermometer is to be expected. A comparision was made between the resistive and magnetic transitions of a high quality $YBa_2Cu_3O_7$ singly crystal. From this we conclude that a temperature uncertainty of 0.2 K should be expected around 100 K. Of course, for lower T_c values, one would expect this uncertainty to be smaller. For Pb and Nb samples the measurements indicate no difference within the accuracy of the thermometry of ±0.05 K. Reproducibility between temperature sweeps is very high. Magnetic transitions taken days apart are indistinguishable.

The magnetic and resistive transitions for the three substitution series are shown in the appropriate sections. One can clearly see the presence of an oxygen isotope shift for all three substitutions. The transitions are at least as sharp as those found in the literature. Some of the magnetic measurements, for the higher concentrations of Pr in particular, show a tail on the high-temperature end of the transition, which makes the determination of T_c somewhat ambiguous. In our previous

work we chose the extrapolation to $R=0$ as the critical temperature not only for the resistive but also for the magnetic transitions. Furthermore, we determined the isotope shift for only one point in the transition. In the present analysis we have used the following procedure for the definition of T_c of the ^{16}O samples and its uncertainty. For resistive measurements we used a linear fit to the transition and chose T_c as the intersection point with the temperature axis. For transitions which show a low-temperature tail, the $R=0$ point and the point of deviation of the data from the linear part of the transition were used as the lower and upper limit of the T_c uncertainty. Otherwise, the uncertainty in temperature (0.2 K near 100 K) was used. For the magnetic transition we also use a linear extrapolation procedure, since it is most likely that the bulk reflects the desired superconducting phase and the small tails are due to impurities. The intersection of the linear extrapolation of the bulk transition back to zero shielding is then defined as T_c. The temperature corresponding to the onset of magnetic shielding was taken as the upper limit of the uncertainty in T_c, while the point of 10% shielding or 0.2 K (the maximum uncertainty in thermometry), whichever is larger, was used for the lower limit. The various T_c's so determined will usually all be different. As a measure of the sharpness of the transitions we also introduce the transition width. For the resistive transitions this was taken as the temperature interval over which a linear fit to the main transition is successful. The width of the magnetic transitions is taken as the temperature interval corresponding to 10 and 90 % of the full signal. Since these transitions are shape dependent, and not all samples have the same size, the magnetic transition widths must be interpreted with caution.

The oxygen isotope shift ΔT_c was determined not just at the defined values of T_c but over the entire top 10% of the magnetic transitions and over about half of the resistive transitions. This was done to investigate the persistence of the isotope shift in the tail section of the transitions. Figure 1 shows the details of the approach to the normal state for a $(Y_{0.7}Pr_{0.2}Ca_{0.1})Ba_2Cu_3O_{7-\delta}$ sample pair in two different representations: the temperature dependence of the normalized magnetization as well as the logarithm of the negative normalized magnetization. The latter emphasizes the tail section and one can clearly see that an isotope shift persists even in this part.

To obtain quantitative values, we used a simple linear fit to the resistive data and ignored the low-temperature tails in the transition. The magnetic transitions were usually normalized (unless noted otherwise) with the fully shielded superconducting state at 0 and the normal state at 1. The discrete data points of the magnetic transitions were then fitted to a smoothly varying function by means of a Simplex[12] least-squares fitting program consisting of three variables. The function used in this Simplex fit is $y=\{[(\ln(t)/t)-e^{-1}]/s\}+1$ for $T<T_c$ and $y=1$ for $T\geq T_c$, where $t=\{e^1+a(T_c-T)]$ and a, s, and T_c are fitting parameters. The fitted curves are shown as solid lines in the detailed graphs of the magnetic transitions (Figs. 1, 4, and 5). The isotope temperature shift ΔT_c between these two curves was then computed for evenly spaced values of the magnetization/susceptibility/resistance. The range was confined to the temperature interval corresponding to the uncertainty in the T_c determination as defined above. In subsequent sections we present representative graphs of the measured magnetic and resistive transitions, the fits to these data and the calculated isotopic temperature shifts. A close inspection of such graphs reveals that an isotope shift persists even in the tail section of the magnetic transitions. Because the ΔT_c values for magnetic measurements are obtained from pairs of points evenly spaced along the magnetic axis, the points well within the tails are not very heavily weighted. Note that the uncertainty in the determination of the isotope shift ΔT_c is much smaller than the uncertainty in the choice of T_c itself.

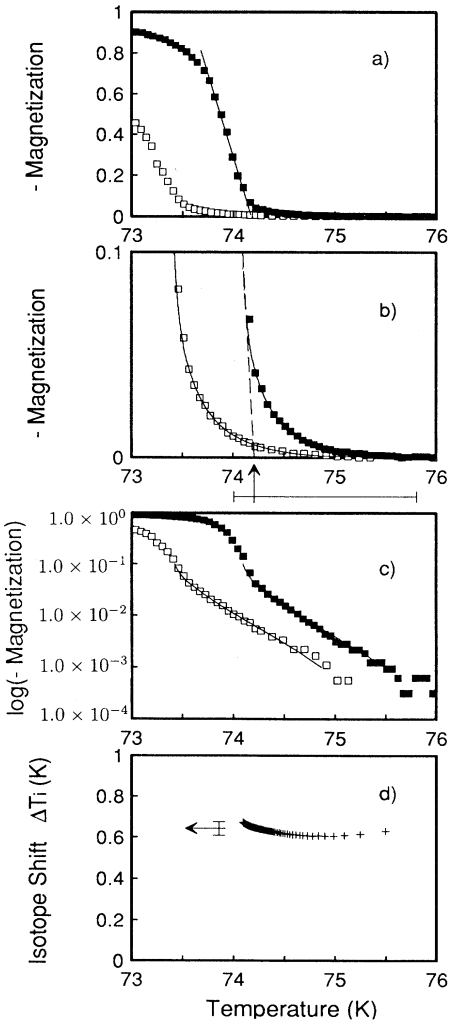

FIG. 1. Magnetic transitions of a $(Y_{0.7}Pr_{0.2}Ca_{0.1})Ba_2Cu_3O_{7-\delta}$ sample pair. (a) shows the bulk of the transition and (b) the approach to the normal state. The arrow indicates the choice of T_c, the bar its uncertainty. (c) The same transition in a semi-log plot emphasizing the tail section. (d) Isotope shifts calculated using Simplex fits to the data above. The arrow points to the mean value, the error bar gives the standard deviation.

PR SUBSTITUTIONS

Measurements of resistance were done at the University of Alberta immediately after the pellets were made. The detailed low-field magnetic measurements were performed by us on small flakes broken off from these pellets. Summary graphs of the transitions of this series were given earlier. While they are quite sharp, the emergence of a high-temperature tail in the magnetic measurements with increasing Pr content can be seen as well as a systematic increase in transition width. T_c as a function of Pr concentration is plotted in Fig. 2 and shows the now familiar depression of superconductivity. The large error bars reflect the extent of the high-temperature tails.

As an example of these transitions, the measurements on the $Y_{0.7}Pr_{0.3}Ba_2Cu_3O_{7-\delta}$ (YBCO) sample pair are presented in Fig. 3. Isotope shifts are clearly present. The procedure for choosing a critical temperature is illustrated by the linear extrapolations of the bulk of the transitions. The details of the high-temperature part are shown in Fig. 4 together with the isotope shift over the temperature range of the transition. The vertical arrows indicate the T_c's obtained by the linear extrapolation method while the horizontal arrows point to the mean isotope shifts calculated using the Simplex fit to the data.

The sample pair with 50% Pr substitution presents a special problem in the analysis of the magnetization measurements. The ZFC curves start to rise immediately at 4.2 K with increasing temperature, especially for the ^{18}O sample. This is due to the inability of these samples to completely shield the field at the lowest measuring temperature (4.2 K). This effect is not very pronounced for the ac-susceptibility curves which were taken with a much smaller measuring field. Clearly, the normalizing procedure should not be used for the magnetization of this sample pair. What is needed are absolute units for magnetization. Due to the different sizes of the flakes

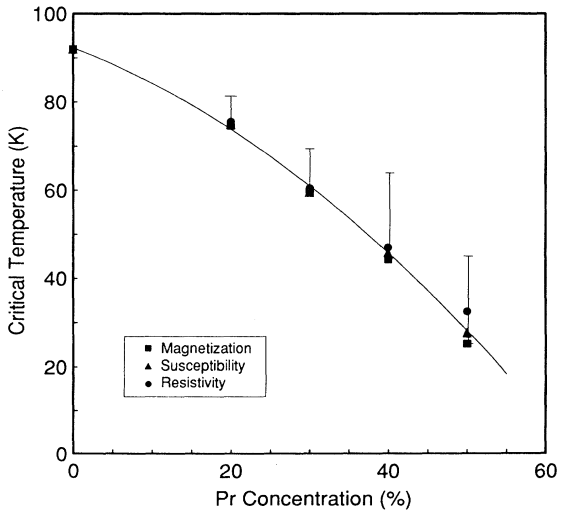

FIG. 2. Critical temperature vs Pr concentration. The solid line is a parabolic fit to the data explained in the text. The error bars reflect mainly the low shielding tails in the magnetic measurements.

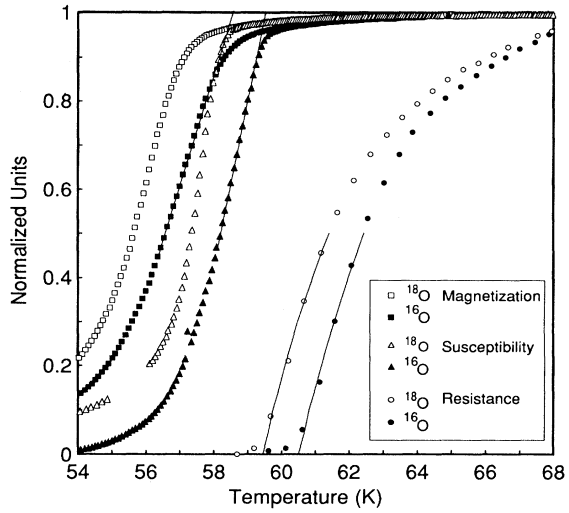

FIG. 3. Normalized transitions of the $Y_{0.7}Pr_{0.3}Ba_2Cu_3O_{7-\delta}$ sample pair. The resistance values are normalized to R(70 K). Solid lines indicate the extrapolation procedure defining the T_c values.

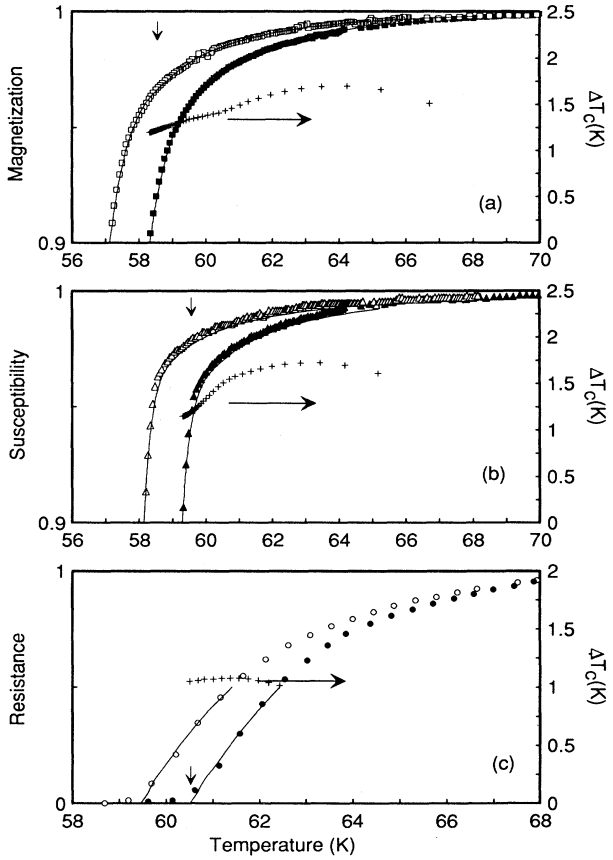

FIG. 4. The $Y_{0.7}Pr_{0.3}Ba_2Cu_3O_{7-\delta}$ sample pair. (a) The high-temperature part of the normalized magnetization and the isotope shift. Vertical arrow: T_c (^{16}O). Horizontal arrow: mean value of ΔT_c. Solid lines: Simplex fit to the data. (b) The same for the normalized susceptibility. (c) Resistive transition normalized to R(70 K) and isotope shift. The vertical arrow represents T_c (^{16}O). The horizontal arrow represents the mean value of ΔT_c.

and the geometry of the pick-up loop, the magnitude of the magnetization can only be estimated. We have come to the conclusion that the isotope shift in magnetization for this sample pair cannot be reliably determined. It is therefore omitted in Table I which gives the critical temperature T_c, the isotope shift ΔT_c and the isotope coefficient α. This point is also absent in Fig. 12 which shows the variation of the isotope shift and isotope coefficient with critical temperature. The resistive transitions for the 50% Pr pair still show vanishing resistance within the sensitivity of the microvoltmeter.

Although tail effects have been reported by other groups, they are not as pronounced as they are in our data. In an attempt to understand these long tails at low shielding, the samples of 20, 30, and 40 % Pr-substituted YBCO were ground into a fine powder and the magnetic measurements performed again. With the small particle size (a few tens of micrometers) in the powder a wider transition is expected. This is indeed the case and the magnetization and susceptibility curves are almost identical. Figure 5 shows the result for the powdered $Y_{0.7}Pr_{0.3}Ba_2Cu_3O_{7-\delta}$ samples and a comparison with the sintered sample flake. However, the long tails at very low shielding remain nearly unchanged. Since we have essentially removed the coupling between individual grains, this broadening must be intrinsic and not due to a weak coupling effect between grains as one might suspect. There is a possibility that the material consists of a number of intermediate phases with a variable range of Pr concentration each having its own T_c and contributing to the total signal. The isotope shifts in the tail should then reflect this variable T_c and should decrease with increasing temperature. However, the observed behavior is ambiguous and no definitive conclusions can be drawn on this point.

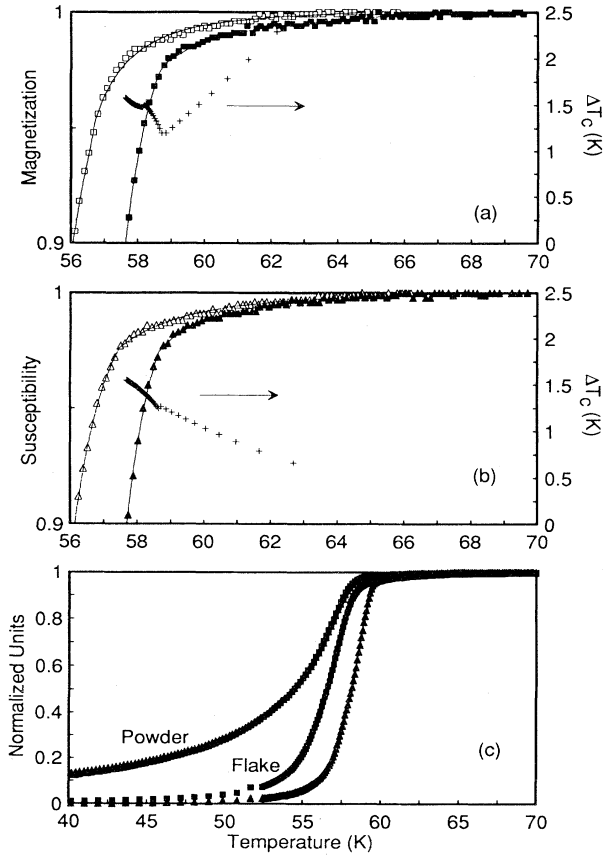

FIG. 5. The $Y_{0.7}Pr_{0.3}Ba_2Cu_3O_{7-\delta}$ sample pair. (a) High-temperature part of the normalized magnetization of powdered material and its isotope shift. The horizontal arrow indicates the mean value of ΔT_c. Solid lines are the simplex fit to the data. (b) The same for the susceptibility. (c) Comparison of the magnetic transitions between flakes and powders.

The isotope shift increases linearly with decreasing critical temperature or increasing Pr concentration as shown in the top half of Fig. 12. However, as we will discuss in the next section, there is also a strong correlation between the isotope shift and the transition width which increases with doping. This greatly complicates the interpretation of the results. Using the measured isotope shifts and a linear extrapolation to 100% ^{18}O content one obtains the dependence of the isotope coefficient α on the critical temperature shown in the bottom half of Fig. 12.

Ca SUBSTITUTIONS IN $(Y_{0.8}Pr_{0.2})Ba_2Cu_3O_{7-\delta}$

The system under investigation here is $(Y_{0.8-y}Pr_{0.2}Ca_y)Ba_2Cu_3O_{7-\delta}$, with $y=0$, 0.05, 0.1, 0.15, 0.2, and 0.25. Initial resistance measurements were performed on the pellets before shaped rods and bars were made from them. Magnetization, both ZFC and FC data, and susceptibility measurements were performed on the rods while resistivity measurements were made on the bars. These Ca samples also exhibit the small ($<3\%$) $BaCuO_2$ impurity line that was seen in the x-ray measurements on the Pr-substituted samples. The measurements of the dc magnetization, the ZFC and FC curves, on the ^{16}O-substituted samples is given in Fig. 6(a). The magnetic and resistive data for all sample pairs are summarized in Figs. 6(b) and 6(c), respectively. T_c as a function of Ca concentration is plotted in Fig. 7. T_c first increases then decreases with a maximum at approximately 10% Ca. The parabolic fits to both this data and the concentration dependence of T_c in the Pr series (Fig. 2) were done with the function, proposed by Neumeier *et al.*,[13] $T_c(x,y)=T_{c0}-A(\gamma-\beta x+y)^2-Bx$, where x is the Pr concentration and y is the Ca concentration. We obtain $T_{c0}=93.6$ K, $A=157$ K, $B=93.3$ K, $\gamma=0.091$, and $\beta=0.874$.

The Meissner fraction decreases then increases with a minimum at 10% Ca. The normal-state resistivity (at $T=83$ K) is also parabolically dependent on the Ca concentration although its minimum is at the slightly higher concentration of 15% Ca. The most obvious effect of the addition of Ca is an increases in the sharpness of the transition and the elimination of the long tails at low shielding. The width of the transition sharpens for all three measurements with the addition of Ca and remains fairly constant with increasing Ca concentration. As with the Pr, the resistance has the narrowest transition and the dc magnetization has the widest.

The critical temperatures, the isotope shifts, and the computed values of the isotope coefficient for all samples in this system are given in Table II. In Fig. 12 we show the variation of α and ΔT_c with T_c. The uncertainty in the temperature values are smaller than those obtained in the Pr series. The measured isotopic shift is similar for both magnetic measurements but the resistivity measurements give a somewhat larger value for the higher concentrations. The isotopic shift ΔT_c and the value of the isotope coefficient, α, change little over the short spread in critical temperature. Due to the large relative uncertainties the functional dependence between the critical temperature and α or ΔT_c is unclear.

The 20% Pr:0% Ca sample made under the same conditions for comparison is quite different from that of the 20% Pr sample discussed in the last section. Its T_c is about 5 K lower than before, the magnetic transition

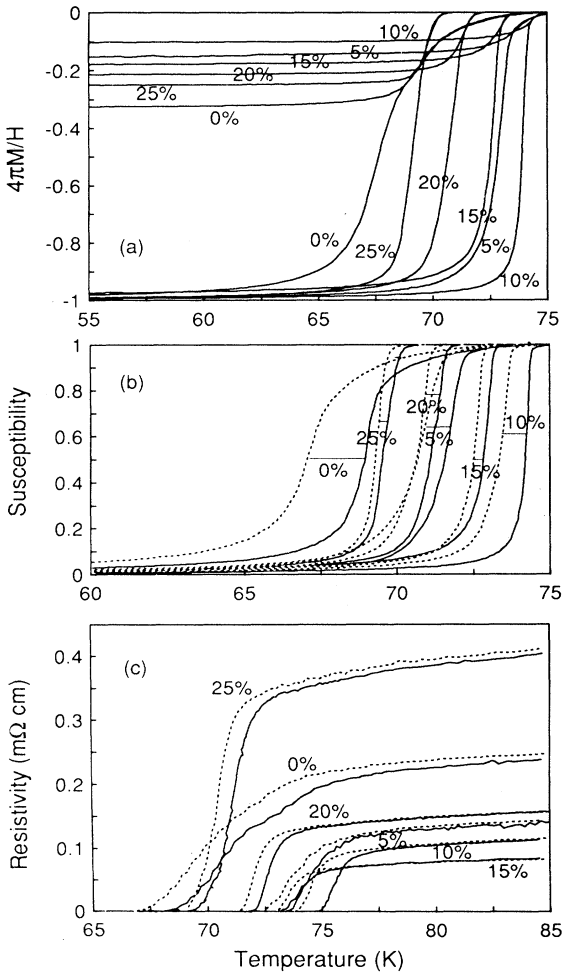

FIG. 6. The transitions for the $(Y_{0.8-y}Pr_{0.2}Ca_y)Ba_2Cu_3O_{7-\delta}$ series. (a) ZFC and FC magnetization curves for the ^{16}O samples. (b) Normalized susceptibility. Solid lines: ^{16}O isotope shift; dashed lines: ^{18}O isotope samples. Corresponding isotope pairs are connected by thin horizontal lines to facilitate identification. (c) Resistivity vs temperature. Solid lines: ^{16}O isotope samples; dashed lines: ^{18}O isotope samples.

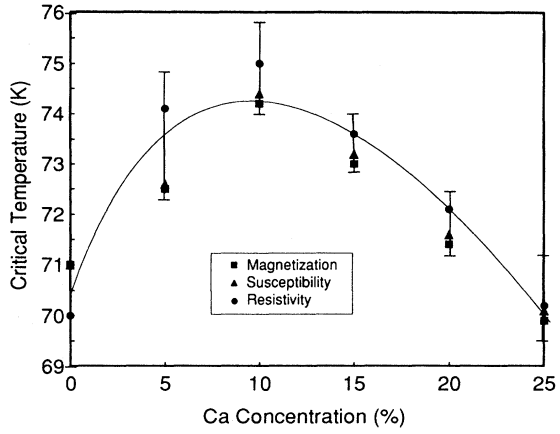

FIG. 7. Critical temperature vs Ca concentration for the $(Y_{0.8-y}Pr_{0.2}Ca_y)Ba_2Cu_3O_{7-\delta}$ series. The solid line is a parabolic fit explained in the text.

width is much broader (~ 1.4 times) and its isotope shift is also larger (~ 1.5 times). Clearly the preparation technique greatly affects the characteristics of the samples. We investigated therefore the relationship between the isotope shift and the width of the transition (Fig. 8) for both the Pr and 20% Pr:Ca-substituted materials. A linear correlation between the isotope shift ΔT_c and the transition width is found. The intercept for a zero-width transition remains finite, in the range of 0.3 to 0.4 K. This surprising result poses the question of whether the measured isotope shift truly depends on the substitutions alone or if some dependence on sample quality has to be taken into account. We discuss this question at the end of this article.

In the Pr system, we noted that the tails in the magnetic measurements become much larger with the increase in Pr concentration as do the transition widths and the isotope shifts. The Ca data, with its much sharper transitions and much reduced low shielding tails, do not exhibit this same effect. As both sets of samples have similar im-

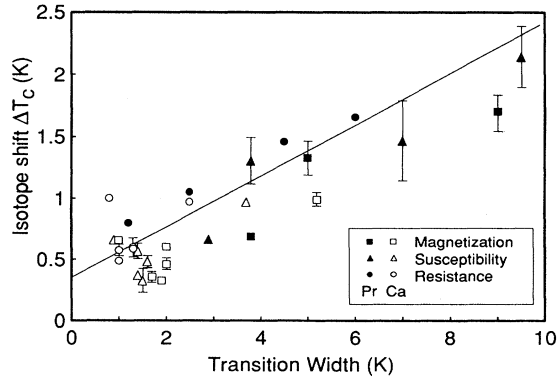

FIG. 8. Isotope shift as a function of the transition width for the $(Y_{1-x}Pr_x)Ba_2Cu_3O_{7-\delta}$ (solid symbols) and $(Y_{0.8-y}Pr_{0.2}Ca_y)Ba_2Cu_3O_{7-\delta}$ (open symbols) series.

purity lines in the x-ray data, it is unlikely that the long tails can be attributed solely to the impurities within the samples.

Zn SUBSTITUTION

The Zn-substituted samples show no impurity lines in the x-ray spectra and they have much sharper transitions than the Pr or Pr:Ca series. The resistivity measurements [Fig. 9(a)] show a smooth drop in the critical temperature with the increase of Zn substitution, from about 70 K at 2% Zn to just under 6 K at 8.5% Zn. These measurements also indicate an increase in the normal state resistivity with increasing Zn concentration.

A summary of the magnetic transitions is shown in Figs. 9(b) and 9(c). Since the samples made for these measurements have all roughly the same shape, demagnetization effects are very similar for all samples. The transitions are quite sharp even for the highest Zn concentrations. Here, the magnetization shows again the presence of tails in the onset of the transition, although not as pronounced as in the Pr substitution series. The high concentration samples have incomplete transitions. This is particularly evident for the 8.5% sample which, when measured resistively, had a good sharp transition with no detectable resistance below 5 K. Figure 9(c) gives a comparison between magnetization and susceptibility transitions for the high concentration range. Again, the transitions are sharp and, when shifted horizontally, can nearly be made to coincide. But the transitions in magnetization are even less complete than those for the susceptibility. Since the measuring field can have an influence on the shape of the transition we investigated this point for the 4 and 7 % Zn concentrations. Figures 10(a) and 10(b) show the ZFC magnetization (normalized to the field) for a range of measuring fields. It is clear that this field has to be chosen as small as possible. Magnetometers requiring several Oe of field can give very broad and incomplete transitions when compared to a low-field instrument. The approach to the normal state

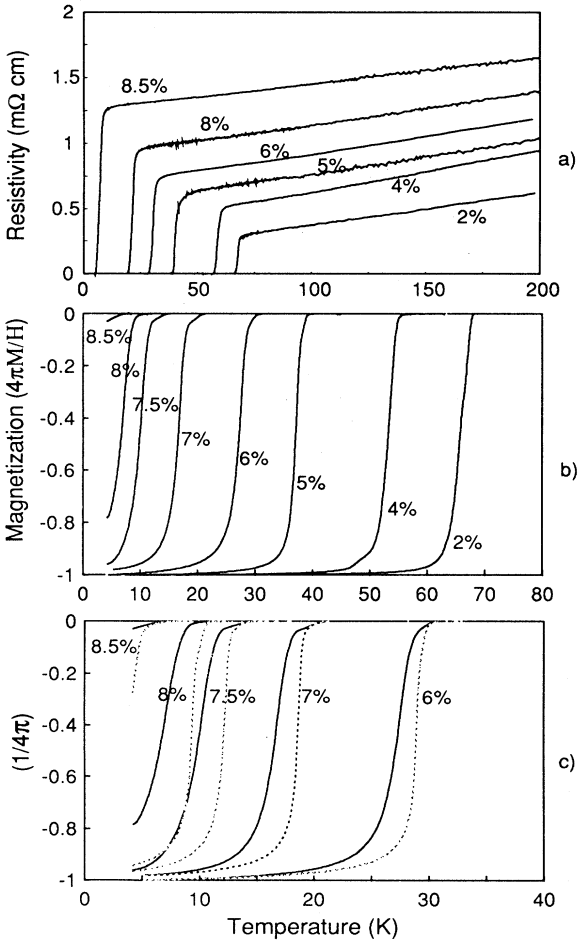

FIG. 9. The transition for Zn-substituted $YBa_2Cu_3O_{7-\delta}$. Only ^{16}O samples are shown. (a) Resistivity, (b) magnetization, and (c) magnetization (solid lines) and susceptibility (dotted lines) for high concentration samples.

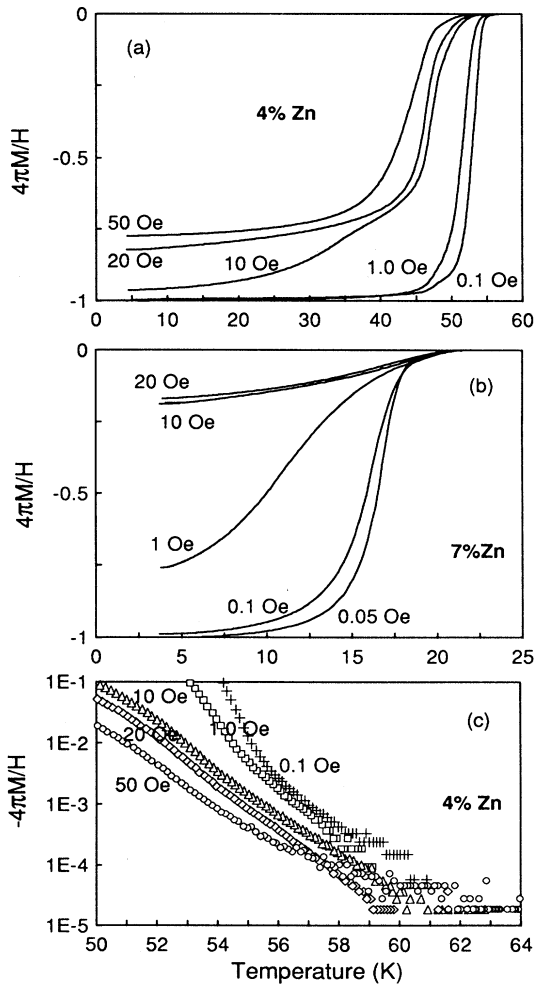

FIG. 10. Field dependence of the transitions in magnetization of ^{16}O samples. (a) 4% Zn substitution, (b) 7% Zn substitution. (c) Semi-log representation for the 4% Zn transitions, emphasizing the approach to the normal state.

for the 7% sample is emphasized in the semi-log presentation of Fig. 10(c). Considering the uncertainty in the zero level it is debatable if there is a field dependence to the onset of the transitions emerging from the noise. But more importantly, we did not find a clear correlation between applied field and the shift in critical temperature and therefore the isotope shift.

The inability of the high Zn concentration samples to shield an applied field to a significant degree has consequences for the determination of the critical temperature and the T_c shift. Since our magnetometer does not give absolute magnitudes, the scaling factor for the magnetization has to be found from calibrations of standard samples and calculations of return-flux corrections as outlined earlier.[11] The calculated magnitudes in the 4.2 K dc susceptibility for the low Zn concentration samples are typically within 10% of $1/(4\pi)$. This means that this uncertainty in the determination of the scaling factors, with the consequent uncertainties of the 4.2 K onset point of the transitions for a low T_c isotope pair, introduces a very large uncertainty in the determination of the isotope shift ΔT_c. A slight vertical scaling change for the magnetization of one member of an isotope pair results in large horizontal ΔT_c changes. We are excluding therefore from our subsequent discussions any magnetic measurements done on a Zn concentration higher than 8%. Resistive measurements on such sample pairs will however be retained, although we have reservations about the validity of isotope measurements where only a fraction of the material is superconducting. We discuss this point below.

There is good agreement throughout this series between the critical temperatures determined by the three different measurement methods. The same is true for the calculated isotope shifts. The difference between T_c obtained magnetically and that obtained resistively is highest for the 4% Zn samples. The transition width remains sharp and independent of the Zn concentration (and critical temperature). This is in contrast to the samples with Pr substitutions. The linear relationship between the critical temperature and the concentration can be seen in Fig. 11. Our results on the resistivity, critical temperature, and the generally narrow transitions involved in Zn substitution agree quite favorably with what exists in the literature.

The critical temperatures and the computed isotope shifts and the isotope coefficients are given in Table III. The isotope shift ΔT_c and the isotope coefficient α, extrapolated to 100% ^{18}O, are plotted against T_c in Fig. 12. The error bars reflect the uncertainties in the T_c determination and the standard deviation from the mean value of ΔT_c obtained by our fitting procedure. The isotope shift appears to decrease slightly with decreasing critical

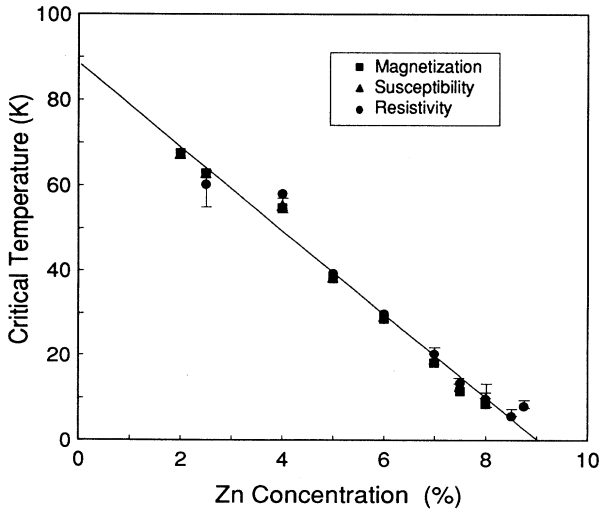

FIG. 11. Critical temperature vs Zn concentration in the $YBa_2(Cu_{1-x}Zn_x)_3O_{7-\delta}$ system.

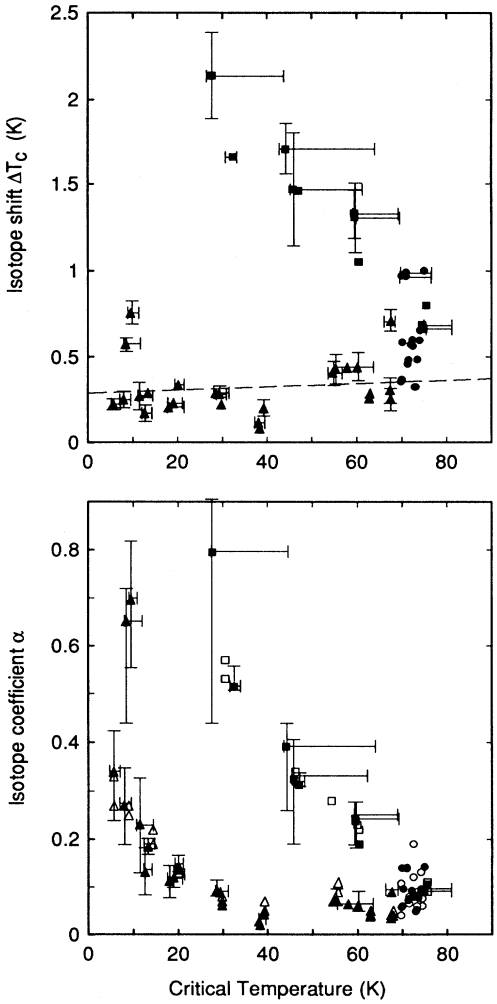

FIG. 12. Top: Isotope shift vs T_c for Pr (squares), Pr:Ca (circles) and Zn (triangles) substituted $YBa_2Cu_3O_{7-\delta}$. A linear fit to the Zn data is shown and discussed in the text. Bottom: Isotope coefficient vs T_c for Pr (squares), Pr:Ca (circles) and Zn (triangles) substituted $YBa_2Cu_3O_{7-\delta}$. Horizontal error bars indicate the uncertainty in the T_c determination due to low shielding tails. Open symbols refer to our previous publications.[4]

temperature which is shown by a linear fit to the data. The scatter in the isotope shift is a measure of the uncertainty one has to expect even for a well behaved system. The isotope coefficient α shows an upturn for the high Zn concentrations. The two points showing a α larger than 0.6 both belong to the 8% samples. Furthermore, the T_c for the 8.5% sample is lower than that for the 8.75% sample. Nevertheless, the resistively determined α follow the general trend with T_c.

DISCUSSION

The results of our oxygen isotope investigation on all three substitution systems are summarized in Fig. 12. What can be seen clearly is that the Pr and Zn substitutions have different effects on the isotope shift and therefore the isotope coefficient α. Increasing Zn concentrations reduce the isotope shift slightly, while the Pr substitutions result in a marked increase in ΔT_c. A comparison in Fig. 12, bottom, with our previously published results[4] must take into account that both the critical temperatures and the isotope shifts were determined in a different way. Also, no attempt had been made to determine the uncertainties in these quantities. Nevertheless, the previously published values for the isotope coefficient α follow very closely the T_c dependence of Fig. 12 with the exception of a few but important high concentration Pr and Zn substitutions. The resistively determined 50% Pr value is very close to what this detailed reevaluation is giving us. However, the value we now obtain from the susceptibility measurement ($T_c=27.7$ K; $\alpha=0.79$) is much larger than quoted earlier ($T_c=30.6$ K; $\alpha=0.57$) but the incomplete magnetic transitions with the large tail make the T_c and ΔT_c determinations very uncertain. The same comment applies to the high Zn substitutions. As we pointed out, we have no confidence in extracting isotope shifts from magnetic transitions that are only a fraction of the expected full shielding value. Consequently, we do not list magnetically determined α values for Zn concentrations beyond 8%. Even the two points ($T_c=8.5$ K; $\alpha=0.65$ and $T_c=9.6$; $\alpha=0.70$) from the 8% Zn sample pair appear to be very large. One must also take into account that resistively determined isotope shifts from samples that contain only a fraction of superconducting phase could be questionable. This concerns the two resistive points with the lowest T_c's belonging to the 8.5 and 8.75 % Zn sample pairs.

One should also keep in mind, that the linear extrapolation to 100% ^{18}O substitution is likely to overestimate the α values. As explained earlier, the difficulty in substituting the O(4) site completely may influence the oxygen isotope effect since phonons involving these oxygens are thought by some to affect superconducting properties. However, a recent study[7] indicates that more than 80% of the oxygen isotope effect is associated with the copper oxide planes. But it is important in future studies to determine the fraction of ^{18}O substitution at the various sites with great accuracy.

Any interpretation of these results must also take into account that for the Pr system (and also for the 20% Pr:Ca system) the isotope shifts and the width of the transitions are correlated as shown in Fig. 8. One must then address the question: is this increase in isotope shift with T_c intrinsic or is it simply a consequence of sample preparation problems associated with increasing Pr substitutions? While we cannot offer an unequivocal experimental answer, there are indications which show that the making conditions must be partially responsible. Consider the two 20% Pr sample pairs which were made under different preparation conditions. Both underwent identical calcining procedures but the sample pair of the original Pr series was sintered at 935 °C for 7 h, while that belonging to the Ca series was held at that temperature for 48 h before undergoing the cooling procedure. The result is that the second ^{18}O sample has a 5 K lower T_c and a magnetic transition that is ~ 1.4 times wider. Clearly, the long sintering process at this elevated temperature, meant to insure complete oxygen isotope substitution, has affected the sample characteristics. But with it goes a 1.5 times larger isotope shift. But we did not always find such a clear-cut correlation between long sintering times at elevated temperatures and sample quality. In a 30% Pr pair a long sintering process did increase the isotope shift by $\sim 14\%$, while it actually sharpened up the transitions slightly. More work must be done on this problem before we can offer a definitive explanation for Fig. 8.

Besides our own work reported here, there are published results of the oxygen isotope effect for substitutions of La for Ba,[14] Fe for Cu,[15] and Co for Cu.[16] They all show a marked upturn in the isotope coefficient α with increasing substitution, very similar to what we find for the substitution of Pr (and Ca) for Y. Unfortunately, these reports do not include enough information to investigate a possible connection between the isotope shift and the width of the transitions. Broad superconducting transitions are usually associated with poor sample quality, and it is not difficult to make an argument that sintered samples like ours contain a good portion of material that is either nonsuperconducting or off stoichiometry (x-ray impurity lines and/or incomplete Meissner fractions, even in powdered samples, can be used as evidence for this). It can then be argued that, whatever the mechanism responsible for superconductivity, isotope shifts could depend on the local environment of the oxygen ions: an intrinsic one due to the bulk superconducting phase and an additional contribution due to the interface between superconducting and normal or insulating phases. The controversy surrounding isotope effect measurements done on samples with broad transition curves can perhaps be resolved when measurements on high quality thin films become available, films thin enough to allow for complete oxygen substitution. Until then, any interpretation of the large increase in α with decreasing T_c seen in our Pr substitution experiments, and perhaps also for the Ba, Fe, and Co substitutions,[14–16] must take into account, that part of this large increase is in all likelihood due to sample problems and could be much smaller.

The Zn-substitution results are much more clearcut. Here, the increase in α at low T_c's is due to the near constant isotope shift at high concentrations. But again,

there are questions concerning the validity of the results at low T_c's. We know from the magnetic measurements that these samples are only partially superconducting. (We do not claim, that a full shielding signal implies that all of the sample is superconducting. But partial shielding definitely indicates the presence of nonsuperconducting material). Zero resistance is observed because a superconducting percolation path can still exist. But again, the situation is similar to the one discussed earlier and the possibility exists, that the oxygen isotope shift is influenced by these nonsuperconducting inclusions.

In conclusion, we have shown in detail how we determine the oxygen isotope coefficient of $Yba_2Cu_3O_{7-\delta}$, substituted with Pr, Ca, and Z, from measurements reported earlier.[4] The criteria used for the determination of T_c and the isotope shift were introduced as well as the uncertainties which are attached to these quantities. This analysis should give confidence, that the experimental results contained in the summary graphs of Fig. 12 are reliable. However, when interpreting these results, one should seriously consider the possibility that the observed increase of the isotope shift with increasing Pr substitution in only partially intrinsic and partially due to nonideal preparation techniques. We have no such reservations for the Zn-substitution system where the transitions remain very sharp even for the highest concentrations and no impurity phases were detected with x-ray diffraction.

ACKNOWLEDGMENTS

We thank J. C. Irwin and E. Altendorf for the Raman investigation, G. I. Sproule for the SIMS measurements, and J. P. Franck, who prepared the samples, for critical comments. The financial support by the National Science and Engineering Research Council of Canada is greatly appreciated.

[1]J. P. Franck, J. Jung, G. Salomons, W. A. Miner, M. A. K. Mohamed, J. Chrzanowski, S. Gygax, J. C. Irwin, D. F. Mitchell, and G. I. Sproule, Physica C **172**, 90 (1990), and references therein.

[2]M. K. Crawford, M. N. Kunchur, S. J. Poon, Phys. Rev. B **41**, 282 (1990).

[3]J. P. Franck, in *Physical Properties of High Temperature Superconductors IV,* edited by D. M. Ginsberg (World Scientific, Singapore, 1994), p. 189.

[4]Pr substitutions: J. P. Franck, S. Gygax, J. Jung, M. A.-K. Mohamed, and G. I. Sproule, Phys. Rev. B **44**, 5318 (1991); J. P. Franck, J. Jung, M. A.-K. Mohamed, S. Gygax, and G. I. Sproule, Physica B **169**, 697 (1991). Pr:Ca substitutions: J. P. Franck, S. Gygax, G. Soerensen, E. Altshuler, A. Hnatiw, J. Jung, M. A.-K. Mohamed, M. K. Yu, G. I. Sproule, J. Chrzanowski, and J. C. Irwin, Physica C **185-189**, 1379 (1991); J. P. Franck, S. Gygax, J. Jung, M. A.-K. Mohamed, and G. I. Sproule, in *High Temperature Superconductivity,* edited by J. Ashkenazi (Plenum, New York, 1991), p. 411; Zn substitutions: J. P. Franck. A. Hnatiw, M. K. Yu, S. Gygax, G. Soerensen, E. Altendorf, and J. C. Irwin, in *Lattice Effects in High-T_c Superconductors,* edited by Y. Bar-Yan, T. Egami, J. Mustre-de Leon, and A. R. Bishop (World Scientific, Singapore, 1992), p. 148.

[5]M. Cardona, R. Liu, C. Thomsen, W. Kress, E. Schönherr, M. Bauer, L. Genzel, and W. König, Solid State Commun. **67**, 789 (1988).

[6]J. C. Irwin, J. Chrzanowski, E. Altendorf, J. P. Franck, and J. Jung, J. Mater. Res. **5**, 2780 (1990).

[7]D. Zech, H. Keller, K. A. Müller, K. Conder, E. Kaldis, E. Liarokapis, and N. Poulakis, Nature (London) **371**, 681 (1994); D. Zech, H. Keller, K. A. Müller, K. Conder, and E. Kaldis, Physica C **235-240**, 1221 (1994).

[8]J. Fink, N. Nücker, H. Romberg, M. Alexander, M. B. Maple, J. J. Neumeier, and J. W. Allen, Phys. Rev. B **42**, 4823 (1990); In-Sang Yang, A. G. Schrott, and C. C. Tsuei, *ibid.* **41**, 8921 (1990).

[9]In-Sang Yang, G. Burns, F. H. Dacol, and C. C. Tsuei, Phys. Rev. B **42**, 4240 (1990); E. Altendorf, J. Chrzanowski, J. C. Irwin, and J. Franck, Solid State Commun. **76**, 391 (1990).

[10]J. P. Franck and D. D. Lawrie, Physica C **235-240**, 1503 (1994).

[11]M. Denhoff, S. Gygax, and J. R. Long, Cryogenics **21**, 400 (1981).

[12]M. S. Caceci and W. P. Cacheris, Byte **9** (5), 340 (1984).

[13]J. J. Neumeier, T. Bjornholm, M. B. Maple, and I. K. Schuller, Phys. Rev. Lett. **63**, 2516 (1989).

[14]H. J. Bornemann and D. E. Morris, Phys. Rev. B **44**, 5322 (1991).

[15]H. J. Bornemann, D. E. Morris, H. B. Liu, A. P. B. Sinha, P. Narwankar, and M. Chandrachood, Physica C **185-189**, 1359 (1991).

[16]J. P. Franck, S. Harker, and M. Yu, Physica B **194-196**, 2087 (1994).